Finite Element Analysis of a Deep Excavation: A Case Study from the Bangkok MRT

Suched Likitlersuang[1*], Chanaton Surarak[2], Dariusz Wanatowski[3]
Erwin Oh[4] and Arumugam Balasubramaniam[5]

1. Associate Professor, Department of Civil Engineering, Faculty of Engineering, Chulalongkorn University, Bangkok, Thailand.
(*Corresponding Author, Email: suched.l@eng.chula.ac.th)
2. Major, Command and General Staff, Royal Thai Army, Thailand.
(Former Ph.D. Student, School of Engineering, Griffith University, Gold Coast Campus, Queensland, Australia) Email: chanatons@gmail.com
3. Associate Professor, Faculty of Science and Engineering, University of Nottingham Ningbo, China. Email: dariusz.wanatowski@nottingham.ac.uk
4. Senior Lecturer, School of Engineering, Griffith University, Gold Coast Campus, Queensland, Australia. Email: y.oh@griffith.edu.au
5. Professor, School of Engineering, Griffith University, Gold Coast Campus, Queensland, Australia. Email: a.bala@griffith.edu.au

Abstract:

Bangkok metropolitan located on thick river soft clay deposit has recently construction project on mass rapid transit underground railway (MRT). This paper presents a finite element study on the Bangkok MRT underground construction project. The Sukhumvit station construction was selected as the case study. The numerical study focus initial input of ground condition and the constitutive soil models. The geotechnical conditions were carried out based on soil investigation report. The parameters of constitutive models were determined and calibrated against the laboratory testing results. Finally, all finite element analysis results are compared with the real field investigations.

Keywords: Deep excavation; Finite Element Method; Mass Rapid Transit; Bangkok Clay

Word number: 7,197

Table number: 9

Figure number: 23

1. Introduction

Geotechnical design and construction on/in soft to very soft soils are usually associated with substantial difficulties. Since these types of soils are sensitive to deformations and possesses small shear strength, they may lead to structural damages during the constriction as well as throughout the life of the projects. This can be from i) excessive settlements or tilting of newly constructed building structures, ii) entrainment settlements of old structures near new erected structures, iii) an adverse effect of excavations on nearby structures, etc (Kempfert & Gebreselassie, 2006).

In Thailand, there is a large river deposit in central plain region called Chao Praya Delta. It is well-known that the delta consists of a broad basin filled with sedimentary soils, especially a thick soft to very soft clay layer on the top deposit. Importantly, Bangkok metropolitan – one of the largest commercial cities in South-East Asia – is also located on the low flat Chao Praya Delta in the Central Plain region of Thailand. There have been several construction projects to improve the quality of infrastructures in the past fifty years. One of the most recent mega construction projects in Bangkok is the Bangkok Mass Rapid Transit (MRT) Underground Railway. This project involves significant geotechnical works especially foundations and excavations.

Nowadays, some commercial FEM codes especially written for geotechnical problem are used to analyse the stability and ground movement due to excavation. Various constitutive soil models, from simple elastic model to mathematically complex non-linear elasto-plastic models have been developed to explain the strength and deformation behaviour of soft soils. However, there is still problem in prediction of movements in and around an excavation with the numerical method. The results of numerical analysis may be influenced by many factors such as simplified geometry and boundary conditions, mesh generation, initial input of ground conditions and significantly the constitutive relationship chosen to model the behaviour of soils.

This research aims to present a simplified two-dimensional finite element studies on deep excavation in soft clays. The Finite Element Code PLAXIS is selected as a numerical tool and the Bangkok MRT underground construction project is chosen as a case study. This study will focus on the effects of mesh generation, initial input of ground condition as well as the constitutive soil models. Finally, all finite element analysis results are compared with the real field investigations.

1.1 Bangkok MRT Project

The first phase of the Bangkok Metropolitan Rapid Transit (MRT) Underground Railway named the Chaloem Ratchamongkhon (or Blue Line) between Hua Lamphong and Bang Sue was operated in 2004. It comprises approximately 20 km of tunnels, constructed using tunnel boring machines (TBM). The route of the MRT Blue Line project is presented in Figure 1. The project was constructed along highly congested roads in the heart of Bangkok city. The tunnel alignment, which is 22 km in length, included 18 underground cut-and-cover underground stations, and was divided into two major sections i.e., the North and South sections (see Figure 1(a)). The underground stations are, typically, comprised of three levels of structure; with the Centre Platform, Side Platform and Stacked Platform as shown in Figure 1(b). The stations are up to 230 m long and approximately 25 m wide, and are excavated up to a depth of 16 m to 32 m below the ground surface. The station perimeter was constructed of diaphragm walls (D-walls), 1.0 – 1.2 m thick and 20 m to 46 m deep. The tunnel lining is of twin bored single-track tunnels. Each tube has an outer diameter of 6.3 m, with an inner diameter of 5.7 m of concrete segmental lining.

A total of 18 underground stations were constructed using the Top-Down construction technique, together with diaphragm walls (D-walls) and concrete slabs as excavation supports. A total tunnel length of 20 km was constructed using eight Earth Pressure Balance (EPB) shields. The excavation depth and D-wall lengths are plotted in Figure 2. The stacked platform stations (S2, S3 and S4) had a greater excavation depth and D-wall length compared to the centre and side-by-side platform stations. The majority of the centre and side-by-side platform stations (except stations S1 and N9) have similar depths of excavation (about 21 – 22 m). However, the embedded depth of the D-wall differed among the South and North contracts due to different design criteria (Phienwej, 2008). More detail on the construction methods for tunnelling and underground stations of the existing MRT Blue Line project can be found in Suwansawat (2002) and Suwansawat et al. (2007).

1.2 Geological Conditions of the Central Plain of Thailand

The Bangkok subsoil forms a part of the larger Chao Phraya Plain and consists of a broad basin filled with sedimentary soil deposits. These deposits form alternate layers of sand, gravel and clay. Field exploration and laboratory tests from both the MRT Blue Line project show that the subsoils, down to a maximum drilling depth of approximately 60 to 65 m, can be roughly divided into: (1) Made ground at 0 – 1m, (2) Soft to Medium Stiff Clays at 1 – 14m, (3) Stiff to Very Stiff Clays at 14 – 26m, (4) First Dense Sand at 26 – 37m, (5) Very Stiff to Hard Clays at 37 – 45m, (6) Second Dense Sand at 45 – 52m and then following by (7) Very Stiff to Hard Clays (see Figure 3 and Figure 10). The aquifer system beneath the city area is very complex and the deep well pumping from the aquifers, over the last fifty years, has caused substantial piezometric drawdown in the upper soft and highly compressible clay layer as presented in Figure 3.

2. Retaining Wall Movements and Ground Settlements Induced by Excavation

2.1 Models for Retaining Wall Displacements and Ground Settlements

The patterns of retaining wall movements are governed by many factors, such as the type of subsoil encountered, the support system of the retaining wall (i.e., braced or anchored), the quality of the workmanship, etc. Ou (2006) categorised the patterns of wall movements as cantilever and deep inward (or braced) excavations as illustrated in Figure 4. At the initial stage of excavation or when the encountered soil is predominantly sandy, a cantilever type of movement tends to occur. As excavation proceeds further and especially in soft soils, deep inward movement is more likely to be encountered.

Further, the ground surface settlement induced by the excavations can be divided into two groups. According to Hsieh & Ou (1998) these are: (i) the spandrel type, in which the maximum surface settlement locates near the wall; and (ii) the concave type, in which the maximum surface settlement occurs at a distance away from the wall. Ou (2006) suggested that the spandrel surface settlement profile is likely to occur with the cantilever pattern of wall movements, while the concave surface settlement profile is likely to occur with a deep inward movement pattern.

2.2 Empirical Predictions for Excavation Induced Ground Movements

The first empirically based method to predict ground settlement, induced by excavation, was proposed by Peck (1969). Using a monitoring database of many case histories, Peck established a relationship between the ground surface settlements, the soil types, the excavated depths, and the workmanship quality. The monitoring data were obtained, in the main, from steel sheet piles or soldier piles; these piles are quite different to those used in more recent construction methods (i.e. diaphragm wall with braced or anchored supports). Indeed, Ou (2006) stated that Peck's method may not necessarily be applicable to all excavation types. Similar to Peck's (1969) method, Clough & O'Rourke (1990) proposed a more refined set of surface settlement envelopes induced by an excavation. The shape and magnitude of the surface settlement envelopes depend on the type of soil, the excavation depth (H_e) and the maximum wall deflection (δ_{hm}).

Hsieh & Ou (1998) further refined Clough & O'Rourke's (1990) method by introducing two zones of influence, namely the Primary Influence Zone (PIZ) and the Secondary Influence Zone (SIZ). The depth of the excavation (H_e) was set as the normalised parameter to predict the length of each zone. The concave settlement profile was proposed as a bi-linear relationship as shown in Figure 5. The surface settlement in the PIZ and SIZ are predicted using Equation (1) and (2), respectively.

$$\delta_v = \left(-0.636\sqrt{\frac{d}{H_e}}+1\right)\delta_{vm}, \quad \text{if } d/H_e \le 2 \text{; and} \tag{1}$$

$$\delta_v = \left(-0.171\sqrt{\frac{d}{H_e}}+0.342\right)\delta_{vm}, \quad \text{if } 2 \le d/H_e \le 4 \tag{2}$$

where δ_v and δ_{vm} are the surface settlement and the maximum surface settlement for the soil at distance d form the wall. To continue the early work of Hsieh & Ou (1998), Ou & Hsieh (2011) suggested new surface settlement patterns, which takes into account not only the excavation depth but also the width of excavation and the depth to hard stratum.

Unlike Peck (1969), and Clough & O'Rourke (1990), where the shapes of the surface settlements are distinguished primarily by soil types, Hsieh & Ou (1998) and Ou & Hsieh (2011) classified the shapes of the surface settlement as spandrel and concave settlement profiles as presented in Figure 4.

3. Bangkok MRT Case Study: Sukhumvit Station

The Sukhumvit station located underneath Asok Road, next to the Sukhumvit – Asok intersection as shown in Figure 6 is selected in this study. The station box is located in the congestion area surrounded by many commercial (3 to 4 stories) and residential buildings. The Sukhumvit station is also a connected station between the MRT underground system and the Bangkok Mass Transit System (BTS) – an elevated train system at Asok station. The soil profile consists of 2 to 3 m of made ground (MG), underlain by approximately 9 m of normally consolidated Bangkok Soft Clay (BSC), with an undrained shear strength of about 20 kN/m^2. The undrained shear strength of this layer tends to increase with depth from the level below 7 m. Beneath the BSC layer, there is 2 m of Medium Clay (MC), with an undrained shear strength of more than 60 kN/m^2. A thin, but continuous, medium dense Clayey Sand (CS) of 1.5 m is sandwiched between the First and Second Stiff Clays (1st SC and 2nd SC), with thicknesses of 6 m and 4 m, respectively. At the depth of 23 to 40 m, the Hard Clay (HC) layer (SPT N values of 30 to 40), with some sand lenses, is found. This HC layer is then underlain by the Dense Sand (DS) layer, up to 60 m deep. The ground water level at this location was found at 1.5 m below the ground surface. A schematic diagram of the Sukhumvit Station soil profile is shown in Figure 7. It is note that this soil profile was developed base on a synthesis series of 4 boreholes of site investigation programme.

3.1 MRT Underground Station Construction

The Sukhumvit Station was constructed using the top down construction method, with a configuration of the centre platform type. The station box had the width, length and depth of 23 × 200 × 21 m. The reinforced concrete diaphragm walls (D-wall) were 1 m thick and 27.9 m deep; they were used for earth-retaining and permanent structures in the station. The 1 m thick concrete slabs of the first, second and third slabs (Roof, Access and Concourse levels) and the 1.8 m thick base slab were the primary braced support system for the D-walls. Figure 6 and 8 show the plan view and the cross section geometry of the Sukhumvit Station. The construction sequences adopted in the station box construction simulation are summarised in Table 2.

3.2 Monitoring System

Extensive instrumentation programs were adopted to monitor the deflection of the diaphragm wall and the ground settlement induced by deep excavations. The instrumentation included inclinometers installed in the D-wall, inclinometers combined with extensometers, surface settlement points, and surface settlement arrays. The building settlement points tilt and crack meters were also installed to ensure that any damage to the adjacent buildings was kept within the design limitations. All instruments and adjacent borehole locations are depicted in Figure 6. These instruments comprise of eight sets of inclinometers installed in the D-wall at various locations and one set of surface settlement arrays (SS1). The surface settlement (SS1) selection for this location was chosen because the surface settlement array (SS1) was located in a bare area between buildings B3 and B4. Thus, the surface settlement measured from the SS1 could be considered as close to a greenfield condition. Moreover, the location of the SS1 was in the middle of the North-South length of the Sukhumvit Station, where the effects of the corners were expected to be minimised. For this reason, the inclinometer number 4 (IN4) will also be used to compare the two-dimensional finite element studies.

3.3 Diaphragm Wall Movements

The field observations from the inclinometers revealed that the cantilever pattern developed after the first excavation stage. As the excavation proceeded to a greater depth, the D-wall showed braced excavation patterns with a bulge in the first stiff clay layer. Figure 9 shows the four stages of the diaphragm wall movements from inclinometers 4, 6 and 8 (IN4, 6 and 8). These inclinometers were located approximately 95, 45 and 11 m from the nearest corner of the excavation box. A significant corner effect occurred on the short side of the excavation box; the maximum wall deflection of IN8 was reduced by half compared to IN4. In contrast, the wall movements of IN6 at all stages only showed a slight reduction (less than 15%) compared to the movements of IN4. At the Sukhumvit Station box, the excavation depth in stage 4 was 21 m. Figure 10 illustrates the maximum wall movements after the stage 4 excavation for all eight inclinometers. It also shows that the corner effect, along both long sides (East: IN2, 5, 7 and West: IN3, 4, 6), is relatively small compared to that of the short sides (North: IN8 and South: IN1).

3.4 Ground Surface Settlements

The measured data of surface settlement at Sukhumvit Station from the surface settlement array (SS1) are plotted as presented in Figure 11. The predicted settlement profiles from empirical methods (Clough & O’Rourke, 1990; Hsieh & Ou, 1998; Ou & Hsieh, 2011) are also presented in Figure 11. All three empirical methods exhibit similar surface settlement envelopes, and are also in good agreement with the field measurements. However, one exception is that, the Clough and O'Rourke's (1990) method cannot predict the surface settlement in the Secondary Influence Zone (SIZ). Additionally, the field surface settlements did not appear to extend far enough from the wall to enable the measurement of the surface settlement in the SIZ. As a result, the findings from the further studies on surface settlements, using finite element analysis, will be compared with both the field measurements (within PIZ) and the predicted surface settlement envelope from the empirical estimation (within SIZ).

4. Finite Element Modelling

The 2D plane strain finite analysis approach, using Plaxis v.9 software (Plaxis 2D v.9 2009), was adopted in this study. As the ratio of the length (*L*) to width (*B*) of Sukhumvit Station box was high (L/B = 8.7), the 3D effect along the long sides of the station (see Figure 6) was small, thus the 2D plane strain approach was considered appropriate. Only the right half of the station box (at the cross section of IN4 and IN5) was modelled because the station configuration was symmetric. A seven-layer soil profile (as shown in Figure 7) was adopted. Importantly, four soil models (i.e., Mohr-Column Model (MCM), Soft Soil Model (SSM), Hardening Soil Model (HSM) and Hardening Soil Model with Small-Strain Stiffness (HSS)) were used to evaluate their performances in deep excavation modelling. All soil layers were modelled using the 15 - node elements. For the structural components (i.e. diaphragm wall, platform and base slab, column and pile), the non - volume plate elements were used. Soil-diaphragm wall interaction was modelled by interface element. The values range from 0.7-0.9 depending the soil profile. The stiffness of the concrete was reduced by 20% to take into account the possibility of cracking (Schweiger, 2009). Table 3 presents the input parameters for the structural components.

4.1 Mesh Generation

Prior to the study on the soil constitutive models, it was decided to clarify the mesh refinement on the finite element model constructed. The finite element models and their mesh generation are shown in Figures 12. The model has an average element size of 2.53 m and a total element number of 649. A finer mesh generation with an average mesh size of 1.42 m and a total of 2054 elements was also adopted in the study. For example, in the case of HSM model analysis, the predicted lateral wall movements and the ground surface settlements reveal the almost identical wall movement profiles and surface settlement envelopes from both models. Therefore, the model with 649 elements was selected for this analysis in order to reduce the calculation time.

4.2 Effect of Initial Pore Water Pressure (Hydrostatic and Drawdown Cases)

As the pore water pressure in the Bangkok area is not hydrostatic, due to the effect of deep well pumping. To investigate the effect of the initial pore water pressure condition in the finite element modelling, two analyses were conducted. The first applied a drawdown pore water pressure profile, while the second assumed a hydrostatic pore water pressure. The ground water level was set at 2.0 m below the ground surface. Figure 3 depicts the drawdown and hydrostatic pore water profiles generated by Plaxis. In a similar manner to the mesh refinement effect study, the all soil parameters, structure element parameters, number of elements in the model were kept the same for both analyses. Only the initial pore water pressure was changed to fit the conditions described.

The results of the finite element analyses, with drawdown and hydrostatic pore water pressure conditions, are shown in Figure 13. For both the maximum lateral wall movement and the maximum surface settlement, the hydrostatic case prediction was two times higher than the corresponding field measurements. The drawdown case seems to give a reasonable agreement, especially for the peak values. More importantly, at the toe of diaphragm wall, the lateral wall movement from the hydrostatic case was nearly three times the values indicated by the inclinometer. This outcome shows a high degree of instability for the diaphragm wall, which did not occur on site. It is, therefore, concluded that a realistic drawdown pore water pressure is necessary for a finite element analysis in the Bangkok area. This drawdown pore water pressure can be then applied to all the analyses in the following sections.

5. Constitutive Soil Models and Their Parameters

The numerical studies of the deep excavation in Bangkok subsoil are often conducted using finite element software with the Mohr-Coulomb model. Many researchers (e.g., Teparaksa, et al., 1999; Phienwej & Gan, 2003; Hooi, 2003; Phienwej, 2008; Mirjalili, 2009) concentrated their work on back calculating the ratio of undrained elastic modulus and undrained shear strength (E_u/s_u). The undrained shear strengths, which are determined from vane shear test in soft clay and triaxial test in stiffer clays, were normally adopted in the back analyses of E_u/s_u ratio. The back analysis results of the E_u/s_u values of Bangkok subsoils are summarised in Table 4.

5.1 Soft Soil Model and Hardening Soil Model

The Soft Soil model (SSM) has been developed within the critical state soil mechanics (CSSM) framework, which is similar to the Cam Clay type soil models.

The SSM utilises the elliptic yield surface as same as the Modified Cam Clay model. However, the Mohr-Coulomb failure criterion is also adopted in the SSM to define the failure line. The 7 parameters for SSM are required to input in Plaxis as summarised in Table 5. More detail on the soft soil model can be found in Brinkgreve (2002).

The Hardening Soil model (HSM) was developed under the framework of the theory of plasticity. The total strains are calculated using a stress-dependent stiffness, in which the stiffness is different in loading and unloading/reloading parts. The strain hardening is assumed to be isotropic, depending on the plastic shear and volumetric strains. A non-associated flow rule is adopted when related to frictional hardening and an associated flow rule is assumed for the cap hardening. A total of 10 input parameters are required in the HSM, as tabulated in Table 5. Schanz *et al.* (1999) explained in detail the formulation and verification of the HSM.

The Soft Soil model (SSM) was actually modified from the Modified Cam Clay (MCC) model. The two main modifications were the use of Mohr Coulomb failure criteria and an improvement in the volumetric yield surface. Parameters λ^* and κ^*, as used in the MCC, remain the same in the SSM. Further two additional parameters, namely ν_{ur} and K_o^{nc}, were introduced. The influences of both the parameters on the triaxial (q versus ε_a and q versus p') and the oedometer (ε_v versus log p') behaviour, resulting from the parametric study, have been discussed in Surarak et al. (2012). Table 6 presents the parameters from the SSM analysis for the BSC, MC, 1stSC, 2ndSC and HC layers. The Hardening Soil Model (HSM) was applied to the MG and CS layers instead of the SSM. The critical state soil model, which forms the basis of the MCC and SSM models, was developed specially to simulate the soft clay behaviour. Therefore, the SSM is not suitable for the MG and CS layers. Also, soil movements owing to excavation of the MG and CS layers are relatively small compared to the BSC, 1stSC and 2ndSC layers. Consequently, using the HSM instead of the SSM in the MG and CS layers will have a negligible influence on this analysis. Parameters λ^* and κ^* were obtained from the consolidation characteristics of the Bangkok clays. Hence, ν_{ur} and K_o^{nc} are set according to the results of the parametric studies. Table 7 presents the parameters from the HSM analysis for the MG, BSC, MC, 1stSC, CS, 2ndSC and HC layers. All soil layers are assumed to have no dilatancy ($\psi = 0^o$). More detail of the parametric studies for Bangkok clays can be seen in Surarak et al. (2012).

5.2 Hardening Soil Model with Small-strain Stiffness (HSS)

The Hardening Soil Model with Small-Strain Stiffness (HSS) is a modification of the Hardening Soil Model, incorporating the small strain stiffness of soils (Benz, 2006). The model employs a modified hyperbolic law of stiffness degradation curve (Hardin & Drnevich, 1972; Santos & Correia, 2001) as in Eq (3).

$$\frac{G}{G_{\max}} = \frac{1}{1 + a\left|\frac{\gamma}{\gamma_{0.7}}\right|} \qquad (3)$$

Two additional parameters, namely the small strain shear modulus (G_{max}), where G = $0.722G_{max}$, and the reference shear strain ($\gamma_{0.7}$), are utilised to govern the soil stiffness at a small strain level. The input parameters for the HSM, as presented in Table 7, remain the same for the HSS analysis. All input parameters of the HSM are carried over to the HSS model, with two additional parameters, namely $G_{\max}$ and $\gamma_{0.7}$ (see Table 5). However, knowledge about the small strain parameters for the MG, SC and HC layers is very limited. Additionally, the expected soil movements arising from these layers are small in comparison to the BSC, MC, 1stSC and 2ndSC layers. Therefore, the HSM is used in the MG, CS and HC layers. The HSS is only applied to the predominant layers, i.e. BSC, MC, 1st SC and 2nd SC layers.

The detailed studies of the small strain parameters, G_{max} and $\gamma_{0.7}$ of the Bangkok Clays were studied (Surarak, 2010). The shear modulus at a small strain (G_{max}) was obtained from both the in-situ tests (down-hole and seismic cone tests) and the laboratory tests using bender elements. Hence, parameter G_{max} is considered to be reliable and is selected straight from the test results, as listed in Table 8. Parameter $\gamma_{0.7}$ is, on the other hand considered to have more variation. The two empirically based methods (Ishibashi & Zhang, 1993; Vucetic & Dobry, 1991) are used to calculate $\gamma_{0.7}$ of the Bangkok Clays, as shown in Figure 14. Both methods estimated similar results for the Bangkok Soft Clay layer, which also coincide with the bender element tests on the Bangkok soft clay (Teachavorasinskul et al., 2002). The two sets of Hardening Soil Models with Small Strain Stiffness analyses (HSS 1 and HSS 2) are considered herein. For the HSS 1 analysis, the average values of $\gamma_{0.7}$ for BSC and MC layers from both the work of Ishibashi & Zhang (1993), and Vucetic & Dobry (1991) are used (see Figure 14). The detail of the small strain stiffness parameters for Bangkok Clays can be found in Surarak (2010).

5.3 Mohr-Coulomb Model (MCM)

The concept of the total stress analysis ($\phi = 0$) with the Mohr-Coulomb model (MCM) for clayey soils has been widely used in geotechnical engineering practice. One of the major advantages of this concept is that the soil parameters are easy to obtain, as only undrained shear strength (s_u) and undrained elastic modulus (E_u) are needed for the rapid loading conditions. The undrained shear strength of the Bangkok subsoils obtained from the vane shear and triaxial tests will be used to govern the strength of the Bangkok Soft Clay (BSC), Medium Clay (MC), 1st Stiff Clay (1st SC), 2nd Stiff Clay (2nd SC), and Hard Clay (HC). Back analyses of the deep excavation problems in Bangkok subsoils (Teparaksa, et al. 1999; Phienwej & Gan, 2003) have shown that the E_u/s_u ratios of 500 and 1000 to 2000 give a reasonable agreement between the measured and the predicted wall movements. In the current study, E_u/s_u of 500 was adopted in the BSC, MC, 1st SC. Higher values of $E_u/s_u = 600$ and 1000 were used for the 2nd SC and HC. These values of E_u/s_u were selected based on previous studies as summarised in Table 4. The MG and CS layers were modelled with the drained analysis. The drained moduli were estimated from the SPT N values from the adjacent boreholes. Table 9 summarises all the parameters used in the MCM analysis.

5.4 Calibrations of Soil Parameters

The stiffness and strength parameters for the SSM and HSM of soft and stiff Bangkok clays have been numerically studied using PLAXIS finite element software (Surarak et al., 2012 and Surarak, 2010). The numerical study was based on a comprehensive set of experimental data on Bangkok subsoils from oedometer and triaxial tests carried out at Asian Institute of Technology as well as the cyclic triaxial tests carried out at Chulalongkorn University. The HSM parameters determined are the Mohr-Coulomb effective stress strength parameters together with the stiffness parameters; tangent stiffness for primary oedometer loading, secant stiffness in undrained and drained triaxial tests, unloading/reloading stiffness and the power for stress level dependency of stiffness. Details can be found in Surarak et al. (2012). In addition, the small strain stiffness parameters for the HSS model of Bangkok Clays were reported in Surarak (2010).

6. Finite Element Result Analysis of the Sukhumvit Station

Finite element analysis of the Sukhumvit Station excavation is studied in this section. Due to symmetrical geometry, one half of the station was modelled (as shown in Figure 12). The calculation steps followed the construction sequences, as tabulated in Table 2. The four stages of the Finite Element Analysis results, where the excavation depths were at 1.5, 7.5, 12.5 and 21 m (Figure 8), were compared with the monitoring data. Note that all the measured data were recorded within one week after the excavation reached the desired levels to retain the undrained condition.

6.1 Results and Discussions on FEA with Mohr-Coulomb Model (MCM)

Figure 15 shows the measured and predicted lateral wall movement and ground surface settlement for the Sukhumvit Station box excavation using MCM. The ground surface settlement predicted by Hsieh & Ou (1998) at the stage 4 excavation was also included for comparison. The predictions given by the MCM analysis slightly under-predict the lateral wall movements at all stages of the excavation. The maximum lateral movement of the wall at the final excavation stage is about 15% lower that the measured value. Contrary to the lateral movement, the MCM analysis shows a much shallower and wider surface settlement profile, when compared to the field measurement and empirical prediction. The predicted maximum surface settlement at the final excavation stage was less than one half of the field measurement. Similar trends in surface settlement profiles of the MCM prediction of surface settlements were found in the literature (Kung et al., 2009 and Schweiger, 2009).

It should be pointed out that wider settlement envelopes, as predicted by the MCM, lead to the overprediction of the surface settlements in the Secondary Influence Zone (SIZ). Nevertheless, a flatter settlement envelope is expected to lead to less predicted differential settlements for the buildings located at the transition of the PIZ and SIZ.

6.2 Results and Discussions on FEA with Soft Soil Model (SSM)

The predicted lateral wall movement profiles and surface settlement envelopes were predicted from SSM analysis are shown in Figure 16. Further, these predicted lateral wall movements at stage 1 to 3 are fairly close to the field measurements. The maximum lateral wall movement at the final stage slightly underpredicted, the measured values by approximately 15 % (similar to MCM predictions). In terms of the ground surface settlement predictions, the SSM gave better trends for the settlement envelope compared to the MCM. Nevertheless, the same general trend of shallower and wider settlement envelopes was observed.

6.3 Results and Discussions on FEA with Hardening Soil Model (HSM)

The strength and stiffness parameters from the study by Surarak et al. (2012) are used as inputs for the HSM analysis in this section. The input parameters listed in Table 7 are the results of the parametric studies and the undrained triaxial test series back-calculations. More specifically, the following procedure is adopted.

(a) The E_{50}^{ref} used in the analyses of drained materials (MG and CS) is estimated from SPT N values of adjacent boreholes. The ratios of $E_{oed}^{ref} = E_{50}^{ref}$ and $E_{ur}^{ref} = 3E_{50}^{ref}$ were suggested by Brinkgreve (2002).

(b) For BSC, MC, 1st SC, 2ndSC and HC, the procedure of triaxial and oedometer modelling are adopted. The triaxial and oedometer tests results from the samples taken from adjacent boreholes were used in stiffness moduli back-calculation.

(c) The parameters ν_{ur}, m and R_f were kept as 0.2, 1 and 0.9, respectively. These values were suggested in Surarak et al. (2012).

Figure 17 compares the measured lateral wall movement and the ground surface settlement with those predicted by the HSM. The predicted lateral wall movements at all excavation stages within the BSC layer (2.5 to 12 m depth) were slightly higher than the field measurements. This overestimation extends further into the deeper layers for the excavation stages 1 to 3. The maximum lateral movement in the last excavation stage (located in 1st and 2nd SC layers) agrees well with the measured values. In the case of the ground surface settlement comparison, the HSM predicted better settlement envelopes compared to those predicted by the MCM and SSM. However, the settlements within the SIZ were still slightly larger than the predictions using the Hsieh & Ou (1998) method.

6.4 Results and Discussions on FEA with Hardening Soil Model with Small-strain Stiffness (HSS)

The results from the HSS 1 analysis are shown in Figure 18. The HSS 1 analysis improved the lateral wall movement prediction, when compared to those predicted by the HSM for all excavation stages in the BSC and MC layers. The predictions about the deeper layers (1st SC, CS and 2nd SC) were, however, much smaller than in the HSM analysis. Indeed, the predicted maximum lateral wall movement was only one half of the measured magnitudes. The corresponding surface settlements were also underpredicted by the HSS 1 analysis. This outcome confirmed that the parameters ($\gamma_{0.7}$) calculated by Ishibashi & Zhang (1993), and Vucetic & Dobry (1991) methods for the BSC and MC layers are valid. However, this conclusion was not true for the Stiff Clay layers. However, there is no information on the laboratory $\gamma_{0.7}$ available in the case Bangkok Stiff Clay. It is suggested that more refined analysis would be appropriate before any definite conclusion can be made on the values of small strain stiffness of Bangkok Stiff Clay, especially when a better set of laboratory and field data is available. For the purpose of this study, it was decided that a back fitted value of $\gamma_{0.7}$ should be adopted.

In the second HSS analysis (HSS 2), only the parameter $\gamma_{0.7}$ in the 1st SC and 2nd SC was adjusted to obtain the best fit results. The best fit value of $\gamma_{0.7}$ for both layers was obtained as 0.002 % (see also Table 8 and Figure 19). The predictions of the wall movements and the surface settlements, obtained by the HSS 2 analysis, are depicted in Figure 19. As far as the results in the final stage are concerned, both the predicted lateral wall movement and the surface settlement agree well with the measured data.

7. Comparisons of Analysis Results

The results from the MCM, SSM, HSM and HSS 2 analyses are compared according to the stage construction in this section. Figures 20 to 23 show the measured and predicted lateral wall movements and surface settlements arising from excavation stage 1 to 4, respectively. As far as the wall movements after the first stage construction are concerned, the SSM, HSM and HSS 2 provide reasonably good predictions compared to the measured data, while the MCM give a slight underpredicted movement. The surface settlement profiles, of all four analyses, are smaller than the field measurements. The maximum surface settlements from the largest to smallest are in the following order: the SSM, HSM, HSS 2 and MCM. The same trends of the predicted wall movements and ground surface settlements are obtained from stage 2 and 3 analyses. The predicted wall movements from the SSM, HSM and HSS 2 analyses are of the same in their magnitudes. Their predictions agree with the measurements at the top part of the D-wall but slightly overpredicted the wall movements from the depth of excavation to the lower end of D-wall. The MCM prediction is, on the other hand, well matches with the measurements at the depth of excavation. However, the MCM analysis gives smaller prediction at the top part of the D-wall. The predicted surface settlements at stage 2 and 3 from the SSM, HSM and HSS 2 analyses are nearly identical. The shapes of their predicted settlement profiles are much steeper than that of the MCM analysis. For the fourth stage of excavation, all the four models give generally good predictions of wall movements. However, the HSS 2 analysis shows the best prediction of maximum wall movement compared to the field data. For the surface settlements, the HSM and HSS 2 show nearly identical settlement profiles. Their results, at the final stage, are also agreeing with the field data. The MCM's settlement profile is much shallower and wider than the measured surface settlement. Its maximum surface settlement is lesser than half of the measured data. The settlement prediction from the SSM lies between the results of the MCM and HSM analyses.

8. Concluding Remarks

This paper investigates the behaviour of D-wall movement and ground surface settlement by means of empirical and numerical analyses. Underground station excavations of Bangkok MRT Blue Line project were used as a case study. Important points based on the results of the study can be summarised as follows.

1) Inclinometer measurements from Sukhumvit Station showed that 3D effects on the long sides of D-wall are small compared to the ones from short sides. This evidence confirmed other studies on 3D effects of deep excavations (Ou et al., 1993).

2) Predicted surface settlement profiles coincided with the observed data within the Primary Influence Zone. However, ground surface settlement measurements did not extend far enough to make comparison in the Secondary Influence Zone.

3) Considerable differences are found from finite element analyses with hydrostatic and drawdown pore water conditions. The case of more realistic drawdown pore pressure predicted closer lateral wall movement and ground surface settlement compared to field observations.

4) In general, better lateral wall movement and ground surface settlement are obtained from higher degrees of sophistication of constitutive models in the following order, i.e. MCM, SSM, HSM and HSS. Nonetheless, no salient differences between the results of axial forces, shear force and bending moment predictions are observed.

5) Back-calculated E_u/s_u ratios from literatures can be used reasonably for lateral movement prediction with MCM. However, accurate ground surface settlements were not obtained.

6) SSM and HSM analyses with soil parameters interpreted from laboratory and in-situ tests (Surarak, et al., 2012), provided better agreement with lateral wall movement and surface settlement field observations.

7) Results from HSS analysis confirmed the values of $\gamma_{0.7}$ in BSC as predicted by Ishibashi & Zhang (1993) and Vucetic & Dobry (1991). In the case of stiff clay, however, a back-calculated $\gamma_{0.7}$ of 0.002% is necessary for better lateral wall movement and surface settlement predictions.

8) As a consequence of this study, it can be stated that no matter what analysis or numerical method is employed, it need not necessarily give a good prediction of ground movements unless the relevant parameters are selected. In the case of the FEM, a suitable simulation process is adopted.

Acknowledgment

The authors wish to thank the late president of the Mass Rapid Transit Authority of Thailand (MRTA), Mr. Chukiat Phota-yanuvat and the MRTA Engineers for their kindness in encouraging and providing relevant data for carrying out academic research activities related to such important works. The first author would like to appreciate research funding from the Stimulus Package 2 (SP2) of Ministry of Education, Thailand under the theme of Green Engineering for Green Society. The second author would like to thank Prof. Suchatvee

Suwansawat (the King Mongkut's Institute of Technology Ladkrabang, Thailand) for his kindness helps during the data collection.

References

Benz, T. (2006). Small-strain stiffness of soils and its numerical consequences. Doctoral Thesis, Institute of Geotechnical Engineering, University of Stuttgart, Stuttgart.

Brinkgreve, R.B.L. (2002). Plaxis 2D – version 8 manuals. A.A. Balkema, Netherlands.

Clough, G. W. and O'Rourke, T. D. (1990). Construction-induced movements of in situ walls, Design and performance of earth retaining structure. ASCE Special Publication, No. 2, pp. 439 – 470.

Hardin, B.O. and Drnevich, V.P. (1972). Shear modulus and damping in soils: design equations and curves. Journal of Soil Mechanics and Foundations Division – ASCE, Vol. 98(SM7), pp. 667 – 692.

Hooi, Y. K. (2003). Ground movements associated with station excavation of the first Bangkok MRT subway. Masters Thesis, Asian Institute of Technology, Thailand.

Hsieh, P.G. and Ou, C.Y. (1998). Shape of ground surface settlement profiles caused by excavation, Canadian Geotechnical Journal, Vol. 35, No. 6, pp. 1004 – 1017.

Ishibashi, I. and Zhang, X. (1993). Unified dynamic shear moduli and damping ratios of sand and clay. Soils and Foundations, Vol. 33, No. 1, pp. 182 – 191.

Kempfert, H. and Gebreselassie, B. (2006). Excavations and Foundations in Soft Soils. Springer-Verlag Berlin Heidelberg, Germany.

Kung, G.T., Ou, C.Y. and Juang, C.H. (2009). Modelling small-strain behaviour of Taipei clays for finite element analysis of braced excavations. Computer and Geotechnics, Vol. 36, No. 1-2, pp. 304 – 319.

Mirjalili, R. (2009). Performance of deep excavations in MRT stations: Bangkok MRT as a case study. Masters Thesis, Griffith University, Australia.

Ou, C.Y., Hsieh, P.G. and Chiou, D. C. (1993). Characteristics of ground surface settlement during excavation. Canadian Geotechnical Journal, Vol. 30, pp. 758 – 767.

Ou, C.Y. and Hsieh, P.G. (2011). A simplified method for predicting ground settlement profiles induced by excavation in soft clay, Computers and Geotechnics 38(12), 987-997.

Ou, C.Y. (2006). Deep excavation: theory and practice. Taylor & Francis, London, UK.

Peck, R.B. (1969). Deep Excavations and Tunnelling in Soft Ground. Proceeding of the 7th International Conference on Soil Mechanics and Foundations Engineering. Mexico City, State of the Art Volume, pp. 225 - 290.

Phienwej, N. (2008). Ground movement in station excavations of Bangkok first MRT. Proceedings of the 6th International Symposium on Tunnelling for Urban Development (IS-Shanghai 2008), Shanghai, China, pp. 181 – 186.

Phienwej, N. and Gan, C. H. (2003). Characteristics of ground movement in deep excavations with concrete diaphragm walls in Bangkok soils and their prediction. Journal of the Southeast Asian Geotechnical Society, Vol. 34, No. 3, pp. 167 – 175.

Plaxis 2D v.9 (2009). Reference Manual.

Santos, J.A. and Correia, A.G. (2001). Reference threshold shear strain of soil: Its application to obtain a unique strain-dependent shear modulus curve for soil. Proceedings of the 15th International Conference on Soil Mechanics and Geotechnical Engineering, Vol. 1, Istanbul, A.A. Balkema, 267 – 270.

Schanz, T., Vermeer, P.A. and Bonnier, P.G. (1999). The hardening soil model: Formulation and verification. Beyond 2000 in Computational Geotechnics. Taylor & Francis, Rotterdam.

Schweiger, H.F. (2009). Influence of constitutive model and EC7 design approach in FEM analysis of deep excavations. Proceeding of ISSMGE International Seminar on Deep Excavations and Retaining Structures, Budapest, pp. 99 – 114.

Surarak, C. (2010). Geotechnical Aspects of the Bangkok MRT Blue Line Project. Ph.D. Thesis, Griffith University, Australia.

Surarak, C., Likitlersuang, S., Wanatowski, D., Balasubramaniam, A., Oh, E. and Guan, H. (2012). Stiffness and strength parameters for hardening soil model of soft and stiff Bangkok clays. Soils and Foundations, Vol. 52, No. 4, pp. 682 – 697.

Suwansawat, S. (2002). Earth Pressure Balance (EPB) shield tunnelling in Bangkok: ground response and prediction of surface settlements using artificial neural networks. Doctoral Thesis, Massachusetts Institute of Technology, USA.

Suwansawat, S., Chaiwonglek, C. and Horny, U. (2007). Design aspects of NATM and cut and cover underground stations for the Bangkok MRTA Blue Line Extension. Proceedings of the 7th International Symposium on Tunnelling for Urban Development (IS-Pattaya 2007). Pattaya City, Thailand, pp. 64 – 75.

Teachavorasinskun, S., Thongchim, P. and Lukkunaprasit, P. (2002). Shear modulus and damping of soft Bangkok clays. Canadian Geotechnical Journal, Vol. 39, No. 5, pp. 1201 – 1208.

Teparaksa, W., Thasananipan, N. and Tanseng, P. (1999). Analysis of Lateral Wall Movement for Deep Braced Excavation of Bangkok Subsoils. Proceeding of the Civil and Environmental Engineering Conference, Bangkok, Thailand, pp. 67 – 76.

Vucetic, M., and Dobry, R. (1991) Effect of soil plasticity on cyclic response. Journal of Geotechnical Engineering, ASCE, Vol. 117, No. 1, pp. 89 – 107.

List of Tables

Table 1: Summary of MRT station dimensions, excavation depths and D-wall lengths

Notation	Station	Station Dimension Length (m)	Station Dimension Width (m)	Excavation Depth, H_e (m)	D-wall Length, L (m)
S1	Hua Lamphong	211	22	15.5	20.1
S2	Sam Yan	178	20	27.1	39.7
S3	Si Lom	154	28	32.6	46.2
S4	Lumphini	230	25	29.6	39.5
S5	Khlong Toei	230	25	21.1	28.6
S6	Queen Sirikit National Convention Center	230	25	23.6	31.6
S7	Sukhumvit	200	23	20.9	27.9
S8	Phetcaburi	199	23	22.4	28.9
S9	Phra Ram 9	400	26	20.9	25.6
N1	Thailand Cultural Centre	358	29	22.4	32.7
N2	Huai Khwang	228	25	21.7	32.2
N3	Sutthisan	228	25	21.7	32.2
N4	Ratchadaphisek	228	25	21.6	34.5
N5	Lad Phrao	293	25	22.0	37.4
N6	Phahon Yothin	228	25	22.0	33.6
N7	Chatuchak Park	364	32	21.8	33.5
N8	Kamphaeng Phet	228	25	22.1	38.5
N9	Bang Sue	228	32	15.8	29.5

Table 2: Construction Sequences of Sukhumvit Station

Sequences	Construction activities
1	Construction of diaphragm walls
2	Construction of bored piles
3	Installation of steel columns, which were plunged into the top of bored piles to form pin piles
4	Pre-excavation and placement of temporary steel decking supported by pin piles for traffic diversion
5	Excavation to level of underside of temporary prop and installation of temporary prop
6	Excavation to level of underside of roof slab and construction of permanent concrete roof slab
7	Removal of temporary prop
8	Excavation to level of underside of second slab level
9	Construction of second concrete slab
10	Stage 8 and 9 were repeated for third and fourth (base) slab
11	Composite columns were installed
13	Backfill roof slab and final road reinstatement

Table 3: Input Parameters for Structure Components

Parameter	Diaphragm wall (1 m thick)	Platform slab (1 m thick)	Base slab (1.8 m thick)	Column (0.8 m dia. @ 11.4 spacing)	Pile (1.8 m dia. @ 11.4 m spacing)
Axial stiffness, EA (MN/m)	28000	28000	50400	1712	3852
Flexural rigidity, EI ($MN/m^2/m$)	2333	2333	13608	91.3	1040
Weight, w (kN/m^2)	16.5	25	45	25	25
Poisson ratio, ν'	0.15	0.15	0.15	0.15	0.15

Table 4: E_u/s_u Ratios Resulted from Finite Element Back Analyses of Previous Studies

Bangkok Soil layers	E_u/s_u ratio			
	Teparaksa et al. (1999)	Phienwej & Gan (2003)	Phienwej (2008)	Mirjalili (2009)
Soft Clay	500	500	500	500
Medium Clay	-	700	-	500
Stiff Clay	2000	1200	1200	500
Hard Clay	-	-	-	1000

Table 5: Soil Models Input Parameters

Input Parameters for: Soft Soil Model (SSM)	Hardening Soil Model (HSM)	Hardening Soil Model with Small Strain Stiffness (HSS)	Parameters	Description	Parameter evaluation
✓	✓	✓	ϕ'	Internal friction angle	Slope of failure line from Mohr-Coulomb failure criterion
✓	✓	✓	c'	Cohesion	y-intercept of failure line from Mohr-Coulomb failure criterion
	✓	✓	R_f	Failure ratio	$(\sigma_1-\sigma_3)_f \,/\, (\sigma_1-\sigma_3)_{ult}$
✓	✓	✓	ψ	Dilatancy angle	Ratio of $d\varepsilon_v^p$ and $d\varepsilon_s^p$
✓			λ^*	Modified compression index	Slope of primary loading curve ln p' versus ε_v space
✓			κ^*	Modified swelling index	Slope of unloading/reloading curve ln p' versus ε_v space
	✓	✓	E_{50}^{ref}	Reference secant stiffness from drained triaxial test	y-intercept in $\log(\sigma_3/p^{ref})$-$\log(E_{50})$ curve
	✓	✓	E_{oed}^{ref}	Reference tangent stiffness for oedometer primary loading	y-intercept in $\log(\sigma_1/p^{ref})$-$\log(E_{oed})$ curve
	✓	✓	E_{ur}^{ref}	Reference unloading/reloading stiffness	y-intercept in $\log(\sigma_3/p^{ref})$-$\log(E_{ur})$ curve
	✓	✓	m	Exponential power	Slope of trend-line in $\log(\sigma_3/p^{ref})$-$\log(E_{50})$ curve
✓	✓	✓	ν_{ur}	Unloading/reloading Poisson's ratio	0.2 (default setting)
✓	✓	✓	K_0^{nc}	Coefficient of earth pressure at rest (NC state)	1-sinϕ' (default setting)
		✓	$G_{\max}^{ref}$	Reference small strain shear modulus	$G_{\max} = G_{\max}^{ref}\left(\dfrac{\sigma_3' + c'\cot\varphi'}{p^{ref} + c'\cot\varphi'}\right)^m$
		✓	$\gamma_{0.7}$	Shear strain amplitude at $0.722G_{\max}$	Modulus degradation curve (plot between $G/G_{\max}$ and log γ)

* p^{ref} is reference pressure (100 kN/m^2)
σ_1 is the major principal stress (kN/m^2)
σ_3 is the minor principal stress (kN/m^2)

Table 6: Parameters for Soft Soil Model (SSM) Analysis

Layer	Soil type	Depth (m)	λ^*	κ^*	ν_{ur}	K_o^{nc}
1	MG	0 – 2.5		HSM		
2	BSC	2.5 – 12	0.12	0.02	0.2	0.7
3	MC	12 – 14	0.1	0.009	0.2	0.6
4	1^{st}SC	14 – 20	0.045	0.009	0.2	0.5
5	CS	20 – 21.5		HSM		
6	2^{nd}SC	21.5 – 26	0.045	0.009	0.2	0.5
7	HC	26 – 45	0.006	0.0009	0.2	0.5

Remarks:

1. Strength parameters (ϕ' and c'), dilatancy angle (ψ) and bulk unit weight for SSM analysis are the same as those of HSM analysis (Table 7)
2. HSM is adopted for Made Ground (MG) and Clayey Sand (CS) layers

Table 7: Parameters for Hardening Soil Model (HSM) Analysis

Layer	Soil type	Depth (m)	γ_b (kN/m^3)	c' (kPa)	ϕ' (^{o})	ψ (^{o})	E_{50}^{ref} (MPa)	E_{oed}^{ref} (MPa)	E_{ur}^{ref} (MPa)	ν_{ur}	m	K_o^{nc}	R_f	Analysis type
1	MG	0 – 2.5	18	1	25	0	45.6	45.6	136.8	0.2	1	0.58	0.9	Drained
2	BSC	2.5 – 12	16.5	1	23	0	0.8	0.85	8.0	0.2	1	0.7	0.9	Undrained
3	MC	12 – 14	17.5	10	25	0	1.65	1.65	5.4	0.2	1	0.6	0.9	Undrained
4	1^{st}SC	14 – 20	19.5	25	26	0	8.5	9.0	30.0	0.2	1	0.5	0.9	Undrained
5	CS	20 – 21.5	19	1	27	0	38.0	38.0	115.0	0.2	0.5	0.55	0.9	Drained
6	2^{nd}SC	21.5 – 26	20	25	26	0	8.5	9.0	30.0	0.2	1	0.5	0.9	Undrained
7	HC	26 – 45	20	40	24	0	30.0	30.0	120.0	0.2	1	0.5	0.9	Undrained

Table 8: Parameters for Hardening Soil Model with Small Strain Stiffness (HSS 1 and 2) Analyses

Layer	Soil type	Depth (m)	G_{max} (MPa)	$\gamma_{0.7}$ (%) for HSS 1	$\gamma_{0.7}$ (%) for HSS 2
1	MG	0 – 2.5		HSM	
2a	BSC 1	2.5 – 7.5	7	0.056	0.056
2b	BSC 2	7.5 – 12	10	0.08	0.08
3	MC	12 – 14	12	0.09	0.09
4	1stSC	14 – 20	30	0.1	0.002
5	CS	20 – 21.5		HSM	
6	2ndSC	21.5 – 26	50	0.1	0.002
7	HC	26 – 45		HSM	

Remarks:

1. Strength parameters (ϕ' and c'), dilatancy angle (ψ) and bulk unit weight for SSM analysis are the same as those of HSM analysis (Table 7)
2. HSM is adopted for Made Ground (MG), Clayey Sand (CS) and Hard Clay (HC) layers

Table 9: Parameters for Mohr-Coulomb Model (MCM) Analysis

Layer	Soil type	Depth (m)	γ_b (kN/m^3)	s_u (kPa)	c' (kPa)	ϕ' (^{o})	ψ (^{o})	E_u (MPa)	E' (MPa)	v	Analysis type
1	MG	0 – 2.5	18	-	1	25	0	-	8	0.3	Drained
2a	BSC 1	2.5 – 7.5	16.5	20	-	-	0	10	-	0.495	Undrained
2b	BSC 2	7.5 – 12	16.5	39	-	-	0	20.5	-	0.495	Undrained
3	MC	12 – 14	17.5	55	-	-	0	27.5	-	0.495	Undrained
4	1stSC	14 – 20	19.5	80	-	-	0	40	-	0.495	Undrained
5	CS	20 – 21.5	19	-	1	27	0	-	53	0.25	Drained
6	2ndSC	21.5 – 26	20	120	-	-	0	72	-	0.495	Undrained
7	HC	26 – 45	20	240	-	-	0	240	-	0.495	Undrained

List of Figures

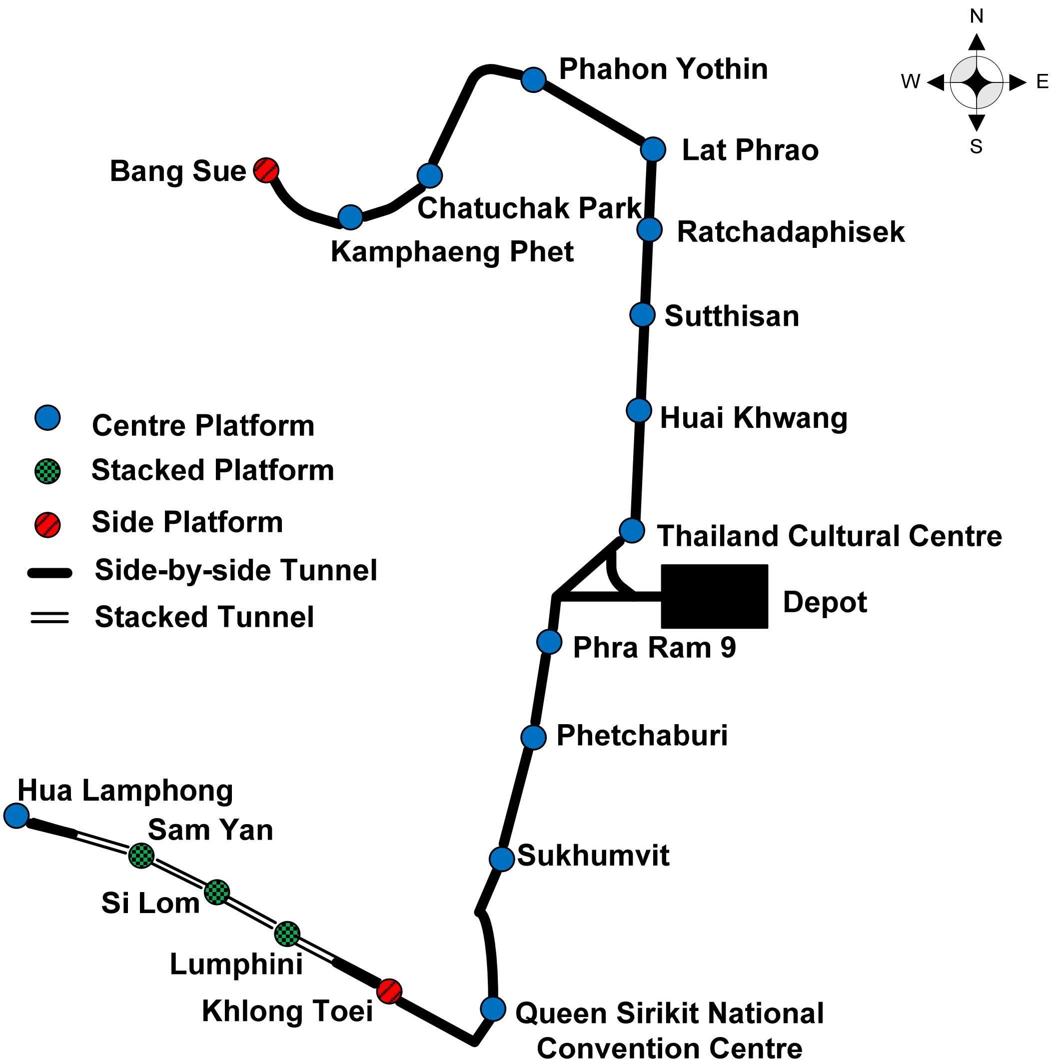

(a) Bangkok MRT Blue Line route

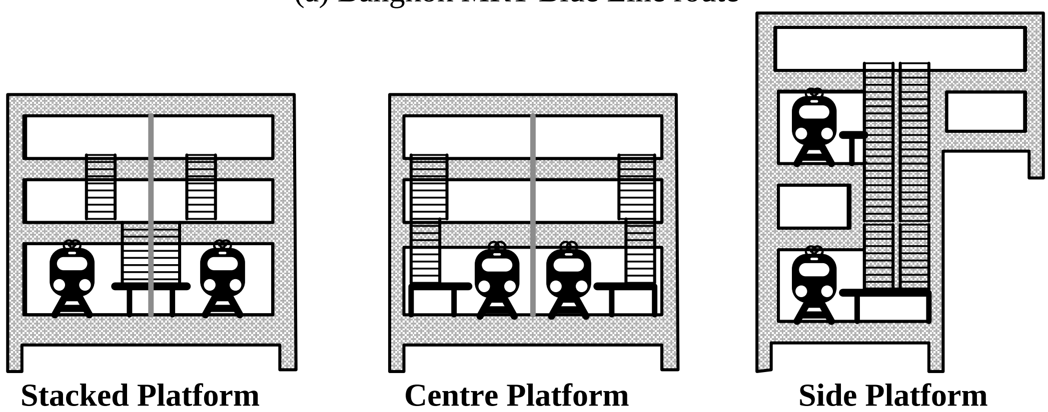

(b) Types of underground stations

Figure 1: Bangkok MRT Blue Line Project

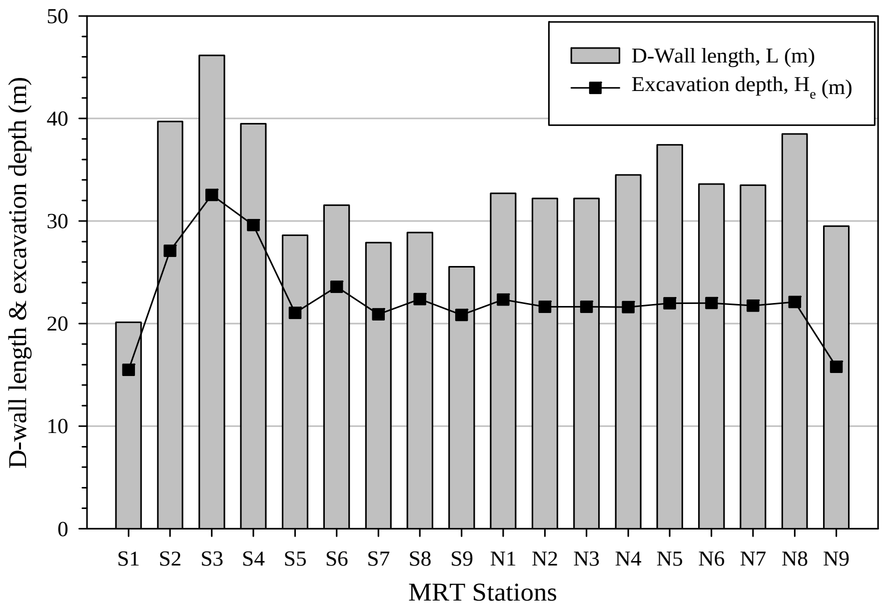

Figure 2: Excavation depth and D-wall length of Bangkok MRT Blue Line stations (after Phienwej, 2008)

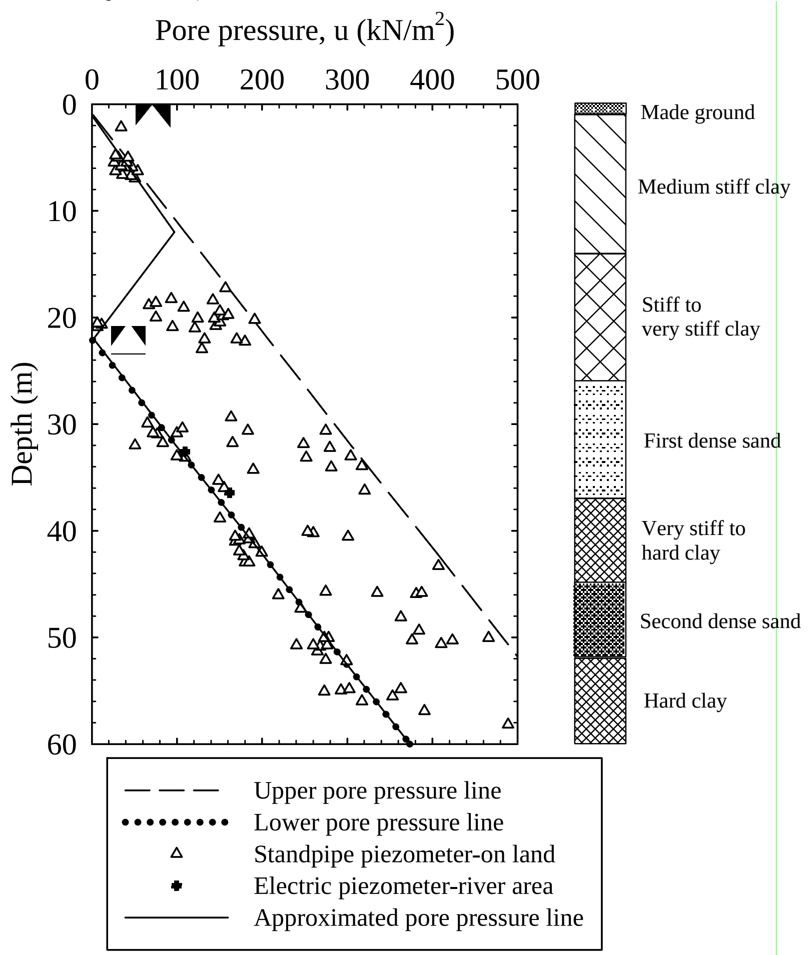

Figure 3: Pore pressure in Bangkok subsoils

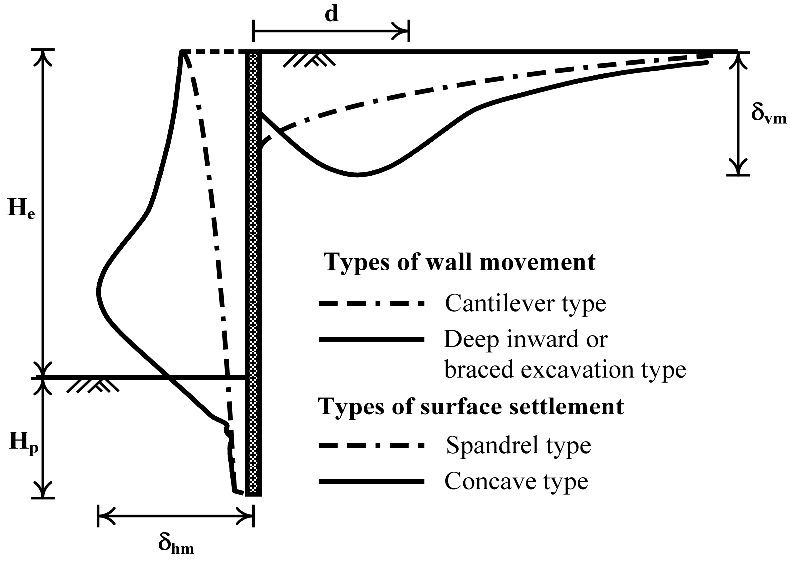

Figure 4: Types of wall movement and ground surface settlement (after Hsieh & Ou, 1998; Ou, 2006)

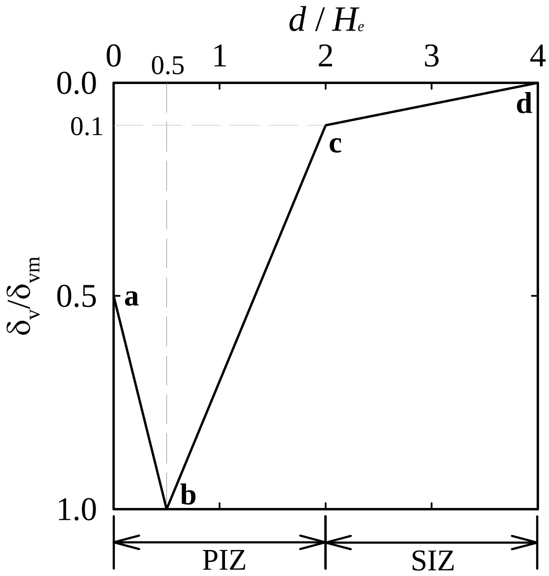

Figure 5: Estimation of ground concave surface settlement (after Hsieh and Ou, 1998)

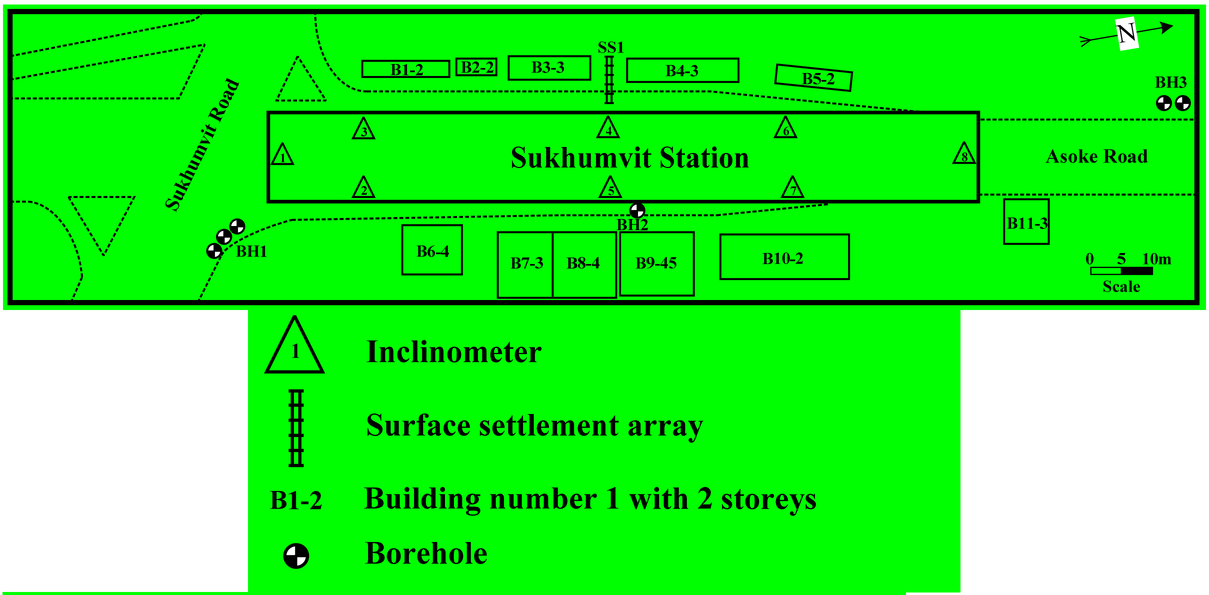

Figure 6: Plan view of the Sukhumvit Station and its instrumentations

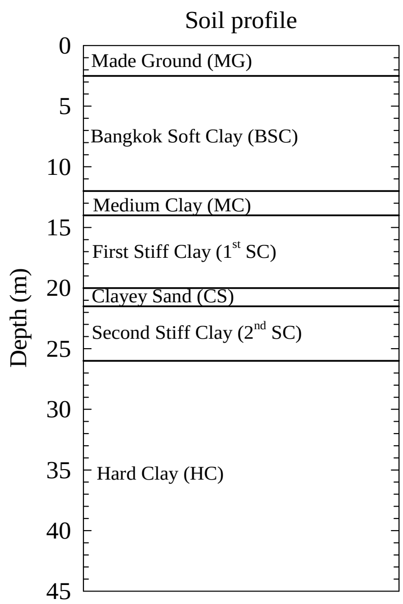

Figure 7: Soil profile at the Sukhumvit station location

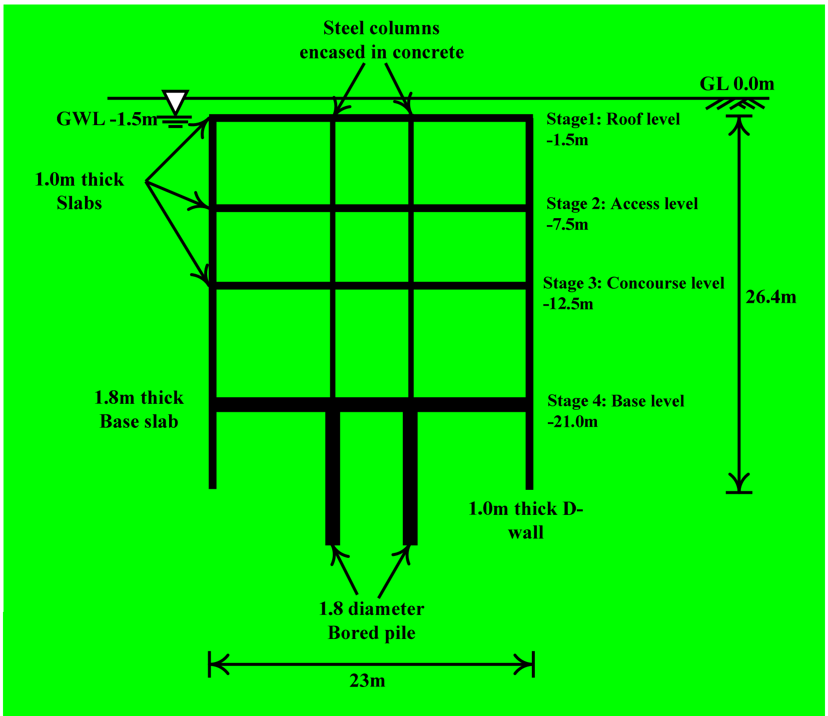

Figure 8: Geometry of Sukhumvit station

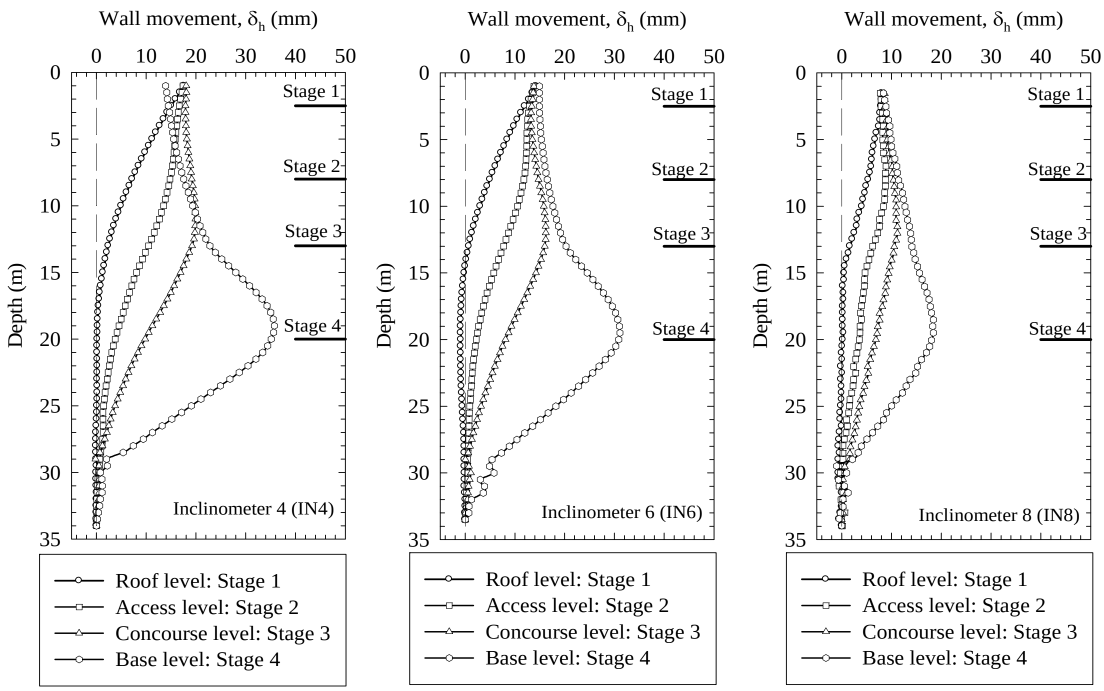

Figure 9: Horizontal movement of diaphragm wall from inclinometers 4, 6 and 8

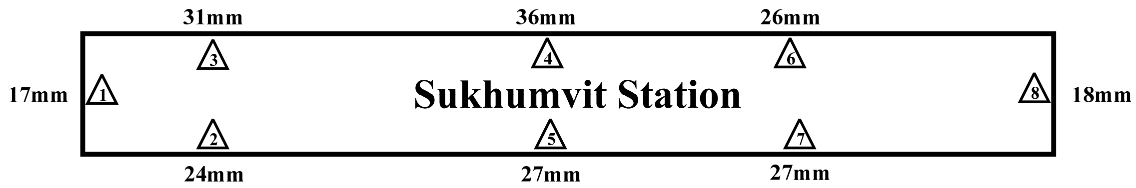

Figure 10: Maximum horizontal movement of D-wall after stage 4 excavation

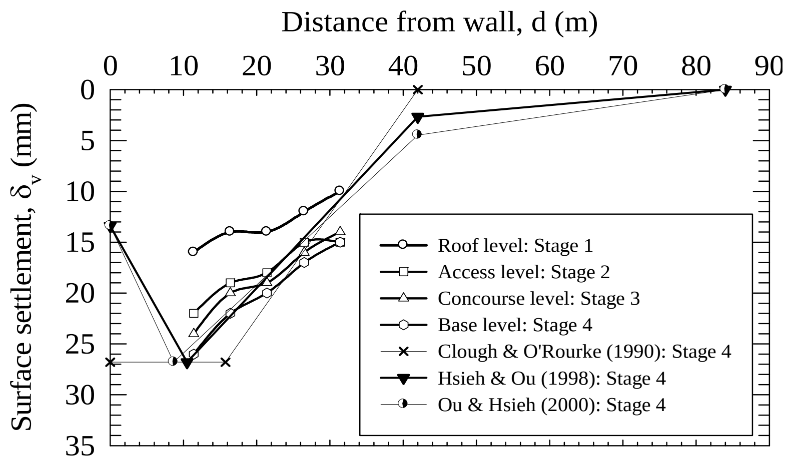

Figure 11: Comparison between measured and predicted surface settlements

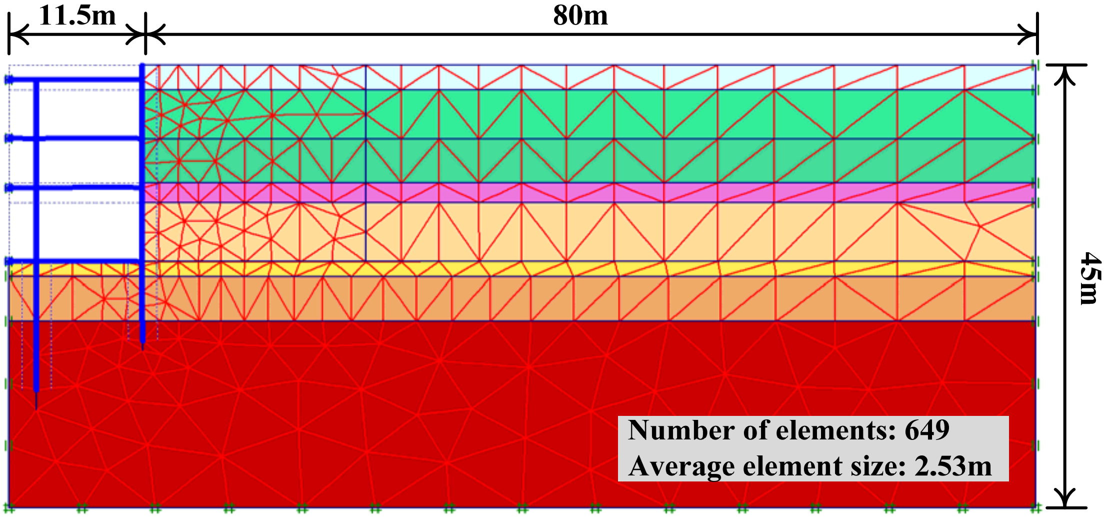

Figure 12: Finite Element Model and Mesh Generation

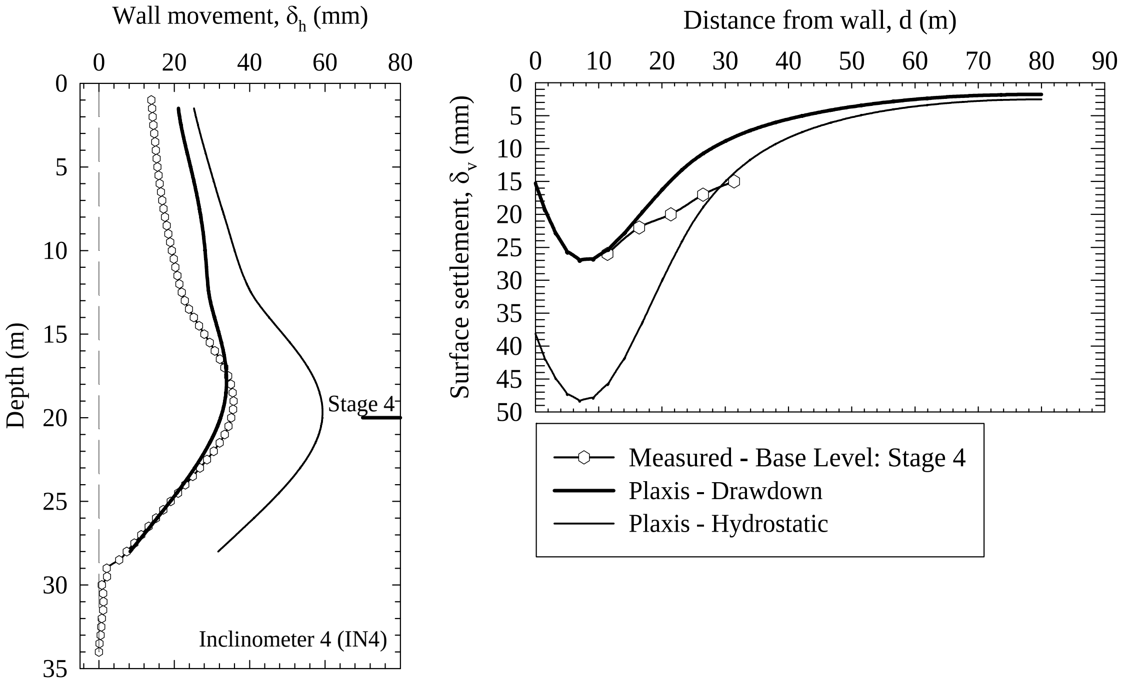

Figure13: Comparison of finite element predictions from drawdown and hydrostatic cases

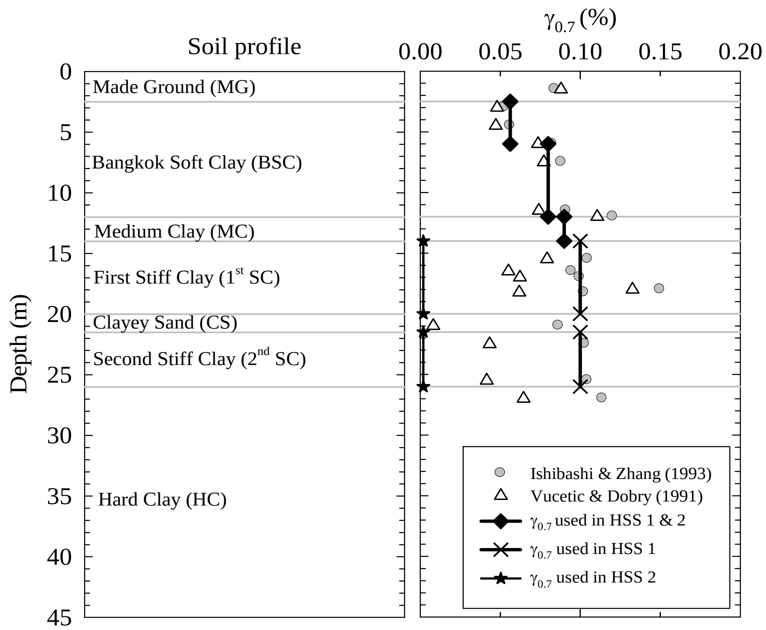

Figure 14: Parameter $\gamma_{0.7}$ as used in HSS 1 and HSS 2 Models

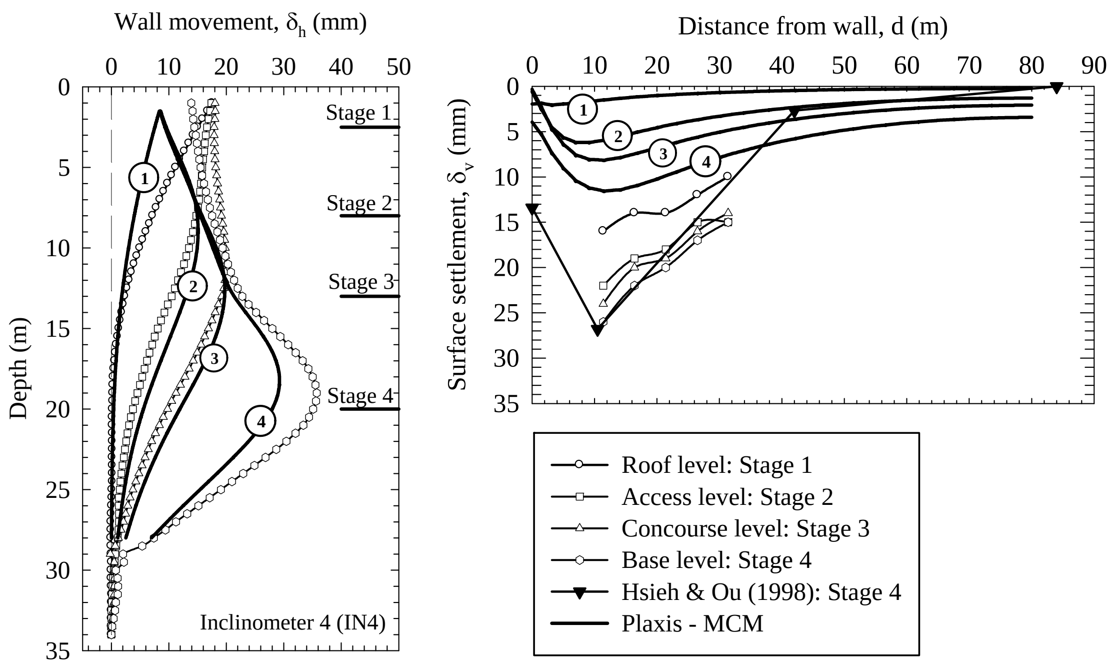

Figure 15: Measured and Predicted Lateral Wall Movement and Surface Settlement from MCM Analysis

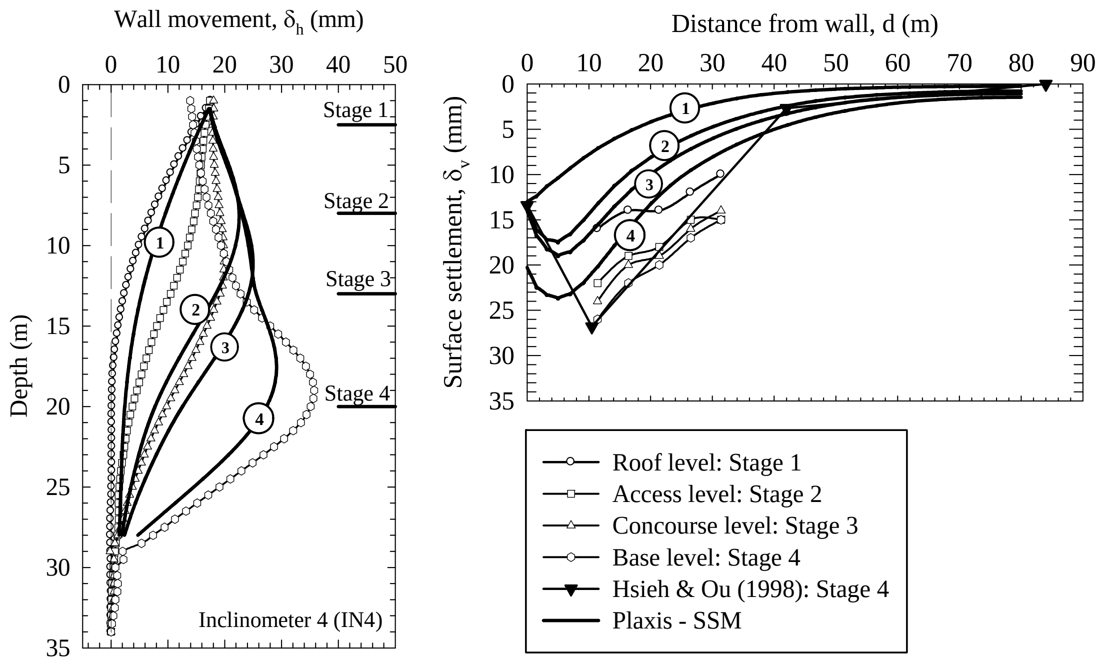

Figure 16: Measured and Predicted Lateral Wall Movement and Surface Settlement from SSM Analysis

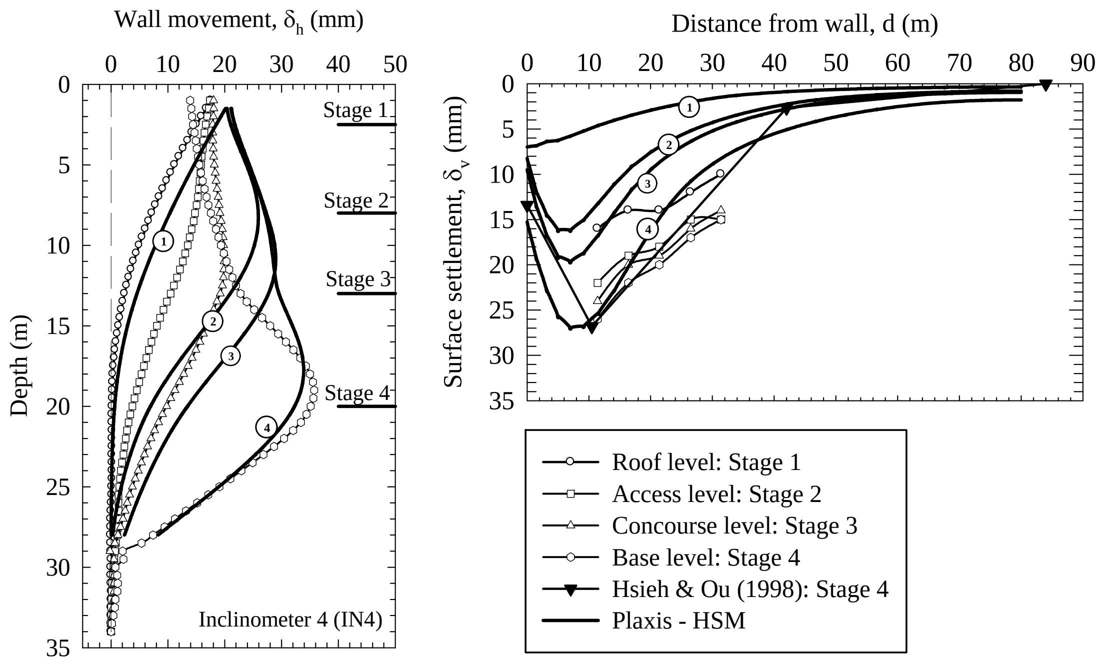

Figure 17: Measured and Predicted Lateral Wall Movement and Surface Settlement from HSM Analysis

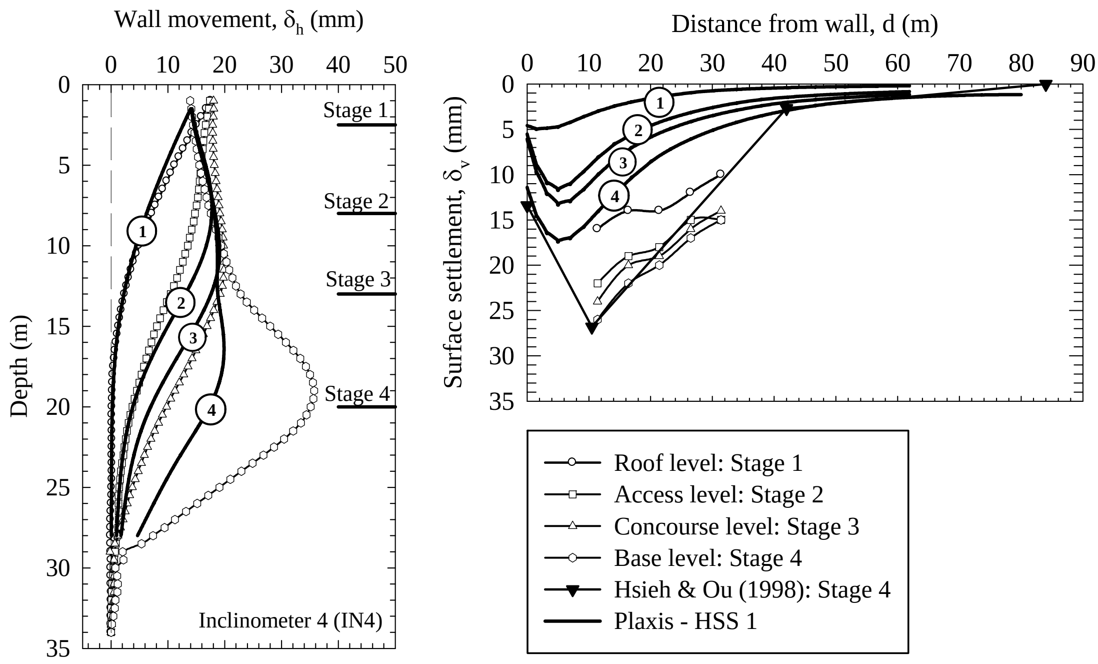

Figure 18: Measured and Predicted Lateral Wall Movement and Surface Settlement from HSS 1 Analysis

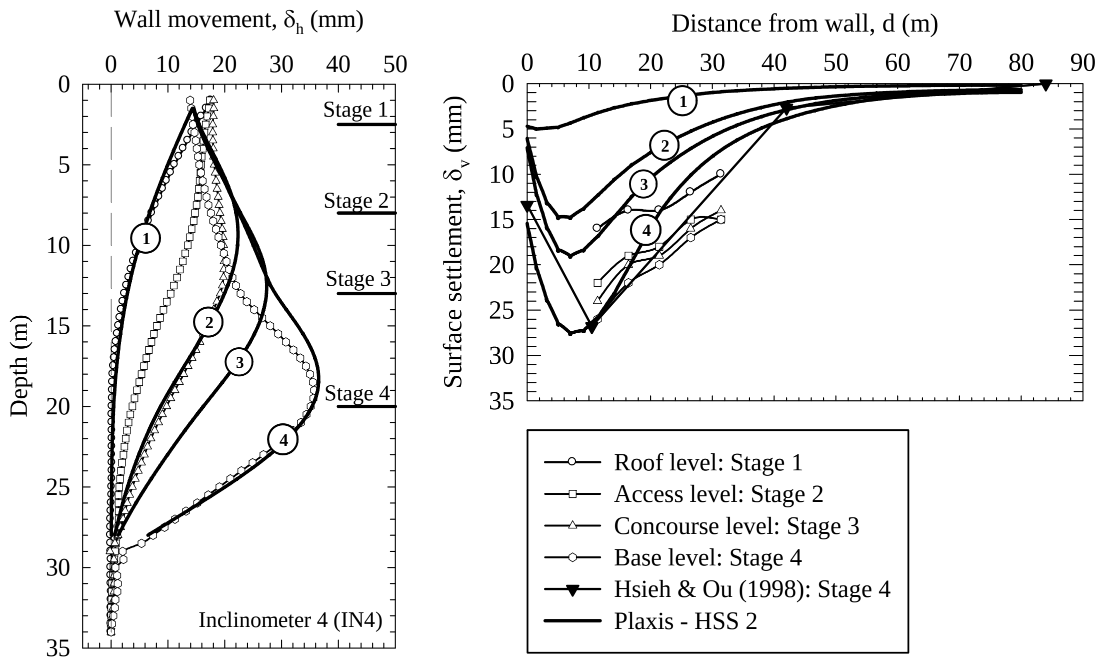

Figure 19: Measured and Predicted Lateral Wall Movement and Surface Settlement from HSS 2 Analysis

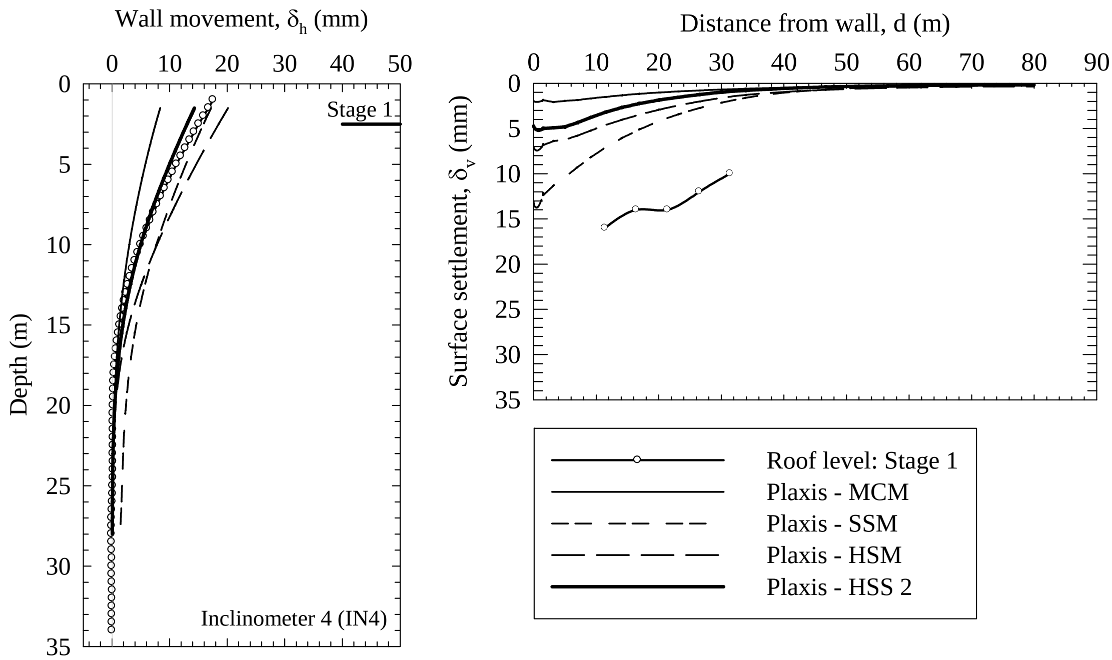

Figure 20: Measured and Predicted Lateral Wall Movement and Surface Settlement at Stage 1 from MCM, SSM, HSM and HSS 2 Analyses

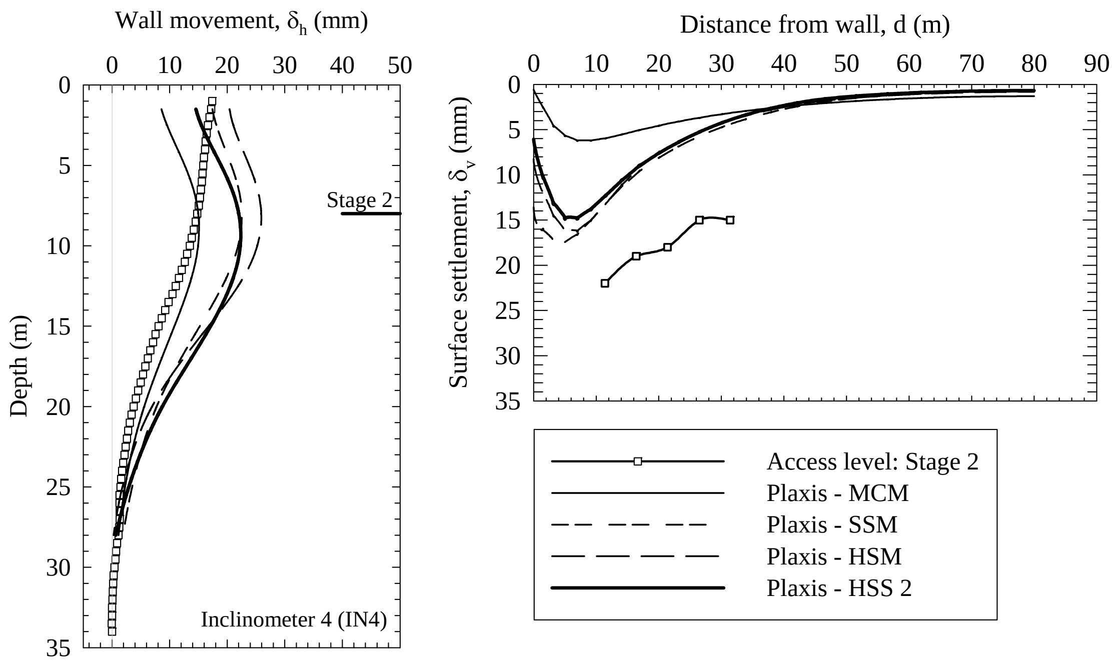

Figure 21: Measured and Predicted Lateral Wall Movement and Surface Settlement at Stage 2 from MCM, SSM, HSM and HSS 2 Analyses

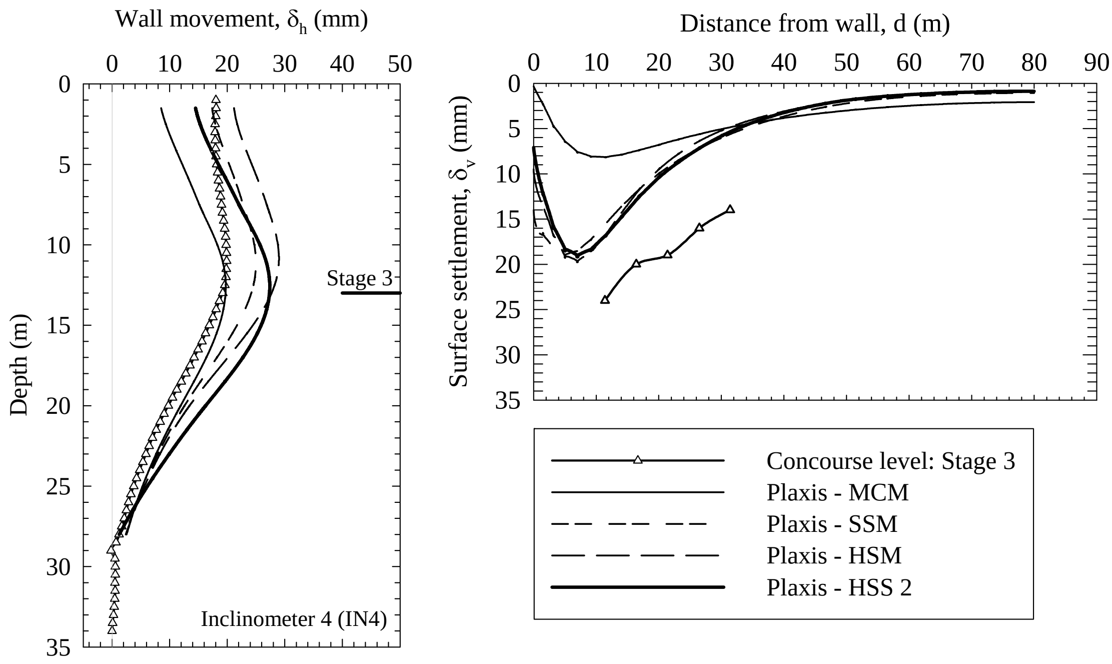

Figure 22: Measured and Predicted Lateral Wall Movement and Surface Settlement at Stage 3 from MCM, SSM, HSM and HSS 2 Analyses

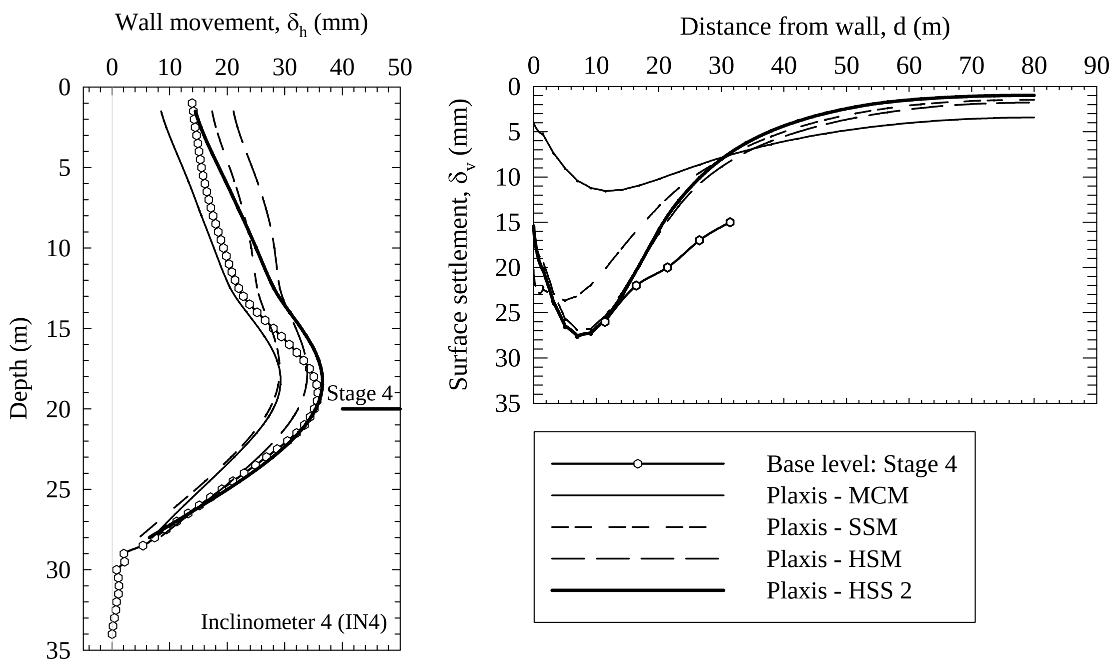

Figure 23: Measured and Predicted Lateral Wall Movement and Surface Settlement at Stage 4 from MCM, SSM, HSM and HSS 2 Analyses